

Orientation-dependent Hydrodynamic Instabilities from Chemo-Marangoni Cells to Large Scale Interfacial Deformations*

SHI Ying(石英)^{a,**} and Kerstin Eckert^b

^a State Key Laboratory of Multiphase Flow in Power Engineering, Xi'an Jiaotong University, Xi'an 710049, China

^b Institute for Aerospace Engineering, Technische Universität Dresden, D-01062 Dresden, Germany

Abstract The interplay between chemistry and interfacial-tension-driven hydrodynamic instabilities has been studied experimentally. The system on hand consists of two immiscible liquids separated along an initially plane interface at which an interfacial reaction takes place to produce *in situ* a surfactant. It is identified that the dynamics of the system depends on the orientation of the Hele-Shaw cell with respect to the vector of gravity. If the Hele-Shaw cell is placed vertically, Marangoni cells with vigorous convection develop in both phases along a nearly planar interface. However, if the Hele-Shaw cell is tilted off the gravity, the instabilities in the system are characterized by the large scale interfacial deformation with a spatio-temporal periodicity together with the chemo-Marangoni convection. The focus is on the exploration of the transition from the cellular mode to the large scale interfacial deformation.

Keywords interfacial reaction, *in situ* produced surfactant, Marangoni convection, interfacial deformation

1 INTRODUCTION

The coupling between chemical reaction and hydrodynamics at interface has attracted increasing interests during the past decades both from the chemical engineering and from nonlinear physics and chemistry. This interest arises both from the large impact of reaction on mass transfer rate and also from the fact that the coupling of chemical kinetics with other transport processes, which often produces patterns of amazing beauty and is far from being fully understood. The fluid properties such as density, viscosity, or surface tension usually vary when composition or temperature change are induced by the chemical reaction. These chemically-induced changes of fluid properties in the bulk or at the interface may result in hydrodynamic instabilities, which exhibit a large variety of convective patterns, such as regular convective structures in the form of fingers, rolls or cells, interfacial waves and interfacial turbulence.

Although numerous studies on liquid-gas systems were devoted to the effect of interfacial turbulence on the adsorption rate[1—4], our focus is entirely on liquid-liquid systems in this work. Experimental evidence in liquid-liquid systems of interfacial convection exhibiting interfacial turbulence has been reported in the literature of reaction of different types. They can be found in liquid-liquid extraction[5,6], hydro-metallurgical extraction of metal ions[7—10], in the photochemical reactions[11] *etc.* Surface deformation plays a crucial role in the nonlinear behaviour of convective patterns, which is responsible for a wide range of interfacial waves. Nakache *et al.*[12] presented such a kind of deformation of interface between aqueous solution of cetyltrimethylammonium chloride and an oil layer containing picric acid, in which a surfactant is dissolved in the aqueous phase and the interfacial tension is changed by the reaction at the interface. This results in pronounced dynamic interfacial deformation, *e.g.* several waves rotating along the

container wall. Since that, it has been attracting a lot of attention and led to more experimental observation. von Gottberg *et al.*[13] employed the similar system as above and the physical motion was observed in and normal to the planar interface, with periodically contracting and twitching cell-like structures at the interface. Kai *et al.*[14,15] studied this kind of instability in a cylindrical and annular glass container. The immiscible liquids are water containing a surfactant and nitrobenzene containing iodine. Depending on the concentration and aspect ratio of the containers they report on the transition between different types of nonlinear wave.

In addition, there are also a number of references reporting the pattern with a high degree of ordering in immiscible liquid-liquid systems with chemical reaction either in the interfacial region or in the bulk phase. Fernandez and Homay[16] reported the viscous fingering in a radial Hele-Shaw cell and compared the finger pattern in reactive and non-reactive systems and put forward that Marangoni stresses are present in reactive systems. Linde and co-workers[17] investigated the pattern formation during an association reaction between monomers and dimers. In square cavities the plane was found to be divided into 2^n sub-squares in which compression-dilatation motions take place as a consequence of Marangoni instability. Moreover, Eckert and Grahn[18] re-examined the systems adopted by Sherwood and Wei with respect to the pattern formation in a Hele-Shaw cell. The resulting self-sustained dynamics and pattern formation in the form of plumes and fingers were suggested to be driven by the coupling between different hydrodynamic instabilities. When NaOH is replaced by another complex base tetramethylammoniumhydroxide, the system displays a regularly organized cellular structures forming in the aqueous phase and slowly penetrating into the bulk. It is proposed that the cellular convection is originated from the lateral difference

Received 2006-12-19, accepted 2007-06-29.

* Supported by Deutsche Forschung Gemeinschaft (Ec/201/1-5) and Deutsches Zentrum fuer Luft und Raumfahrt (50WM0058).

** To whom correspondence should be addressed. E-mail: shiying@mail.xjtu.edu.cn

in buoyancy[19]. If such system is put in a horizontal Hele-Shaw cell, this sort of structure completely vanishes in favor of a planar reaction front[20].

In the present paper a chemical system displaying different sorts of Marangoni instabilities depending on the tilting angle of the Hele-Shaw cell is reported. Our aim is to describe how the change in the effective gravity affects the convective instabilities and especially focus on the particular role of Marangoni instabilities in chemo-convective patterns.

2 EXPERIMENTAL SECTION

2.1 Chemical system

The system to be studied is a quasi-two-dimensional configuration of two immiscible liquid phases in contact along a plane interface. *n*-Hexane (density $\rho = 0.659 \text{ g}\cdot\text{ml}^{-1}$, kinematic viscosity $\nu = 0.5 \times 10^{-6} \text{ m}^2\cdot\text{s}^{-1}$), into which myristoyl chloride was dissolved, acts as the organic phase. Potassium hydroxide was dissolved in the water to form the aqueous phase. Myristoyl chloride (henceforth abbreviated to MyCl, purity >99%) was purchased from Fluka while all other chemicals were purchased with the highest purity from AcrosOrganics. The reaction takes place immediately after contact of both phases. It comprises two main steps. First, the relatively slow base catalyzed hydrolysis of MyCl to myristic acid and second, the neutralization of the latter by KOH to form the soap, potassium myristate (P-My). Both the intermediate and the final products are surface-active species, which reduce the interfacial tension. The measurements of the interfacial tension change with the concentration, *i.e.* the surface activity, have shown that P-My is the stronger surfactant compared with myristic acid. The dependence of the equilibrium surface tension, σ , of P-My in $0.5 \text{ mol}\cdot\text{L}^{-1}$ KOH aqueous solution on P-My concentration was determined by means of the Wilhelmy plate method using a KSV Sigma 700 tensiometer and the curve is plotted in Fig. 1. The surface tension decreases continuously as the concentration increases up to about $0.001 \text{ mol}\cdot\text{L}^{-1}$. Then it stays approximately constant at $31.7 \text{ mN}\cdot\text{m}^{-1}$ independently of any further increase in concentration. Thus, the critical micelle concentration (CMC) is achieved at approximately $1\text{--}2 \text{ mmol}\cdot\text{L}^{-1}$ of P-My. In the experiments the initial concentrations of MyCl, C_{M_0} , and KOH, C_{B_0} , vary between $0.1 \text{ mol}\cdot\text{L}^{-1}$ and $0.5 \text{ mol}\cdot\text{L}^{-1}$ and are, in the rule, significantly above the CMC for P-My.

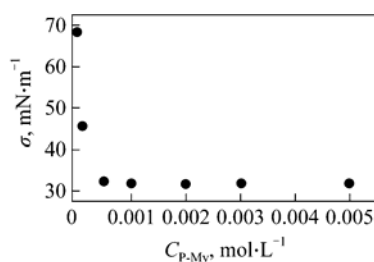


Figure 1 Measurement of the equilibrium surface tension of $0.5 \text{ mol}\cdot\text{L}^{-1}$ KOH aqueous solution exposed to air as a function of P-My concentration

2.2 Experimental setup

All experiments are performed in a Hele-Shaw cell (abbreviated to HS cell). It consists of two transparent borosilicate glasses of optical quality with a narrow gap ($b = 0.5 \text{ mm}$) spaced by Teflon foil, in which the liquid-liquid system is placed. Thus formed fluid chamber is 120 mm high and 60 mm wide. The glass plates are mounted on viton gaskets in aluminium frames screwed together. The teflon foil mentioned above acts not only as the spacer but also seal between the glass plates. A principal sketch of the system is shown in Fig. 2. The cell is filled by means of syringes through bores in the glass plates. First, the aqueous phase, then followed by the organic phase, as schematically illustrated in Fig. 2. It guarantees a liquid-liquid contact without noticeable shear flow within 1–2 seconds. For the details we refer to Refs.[20] and [21].

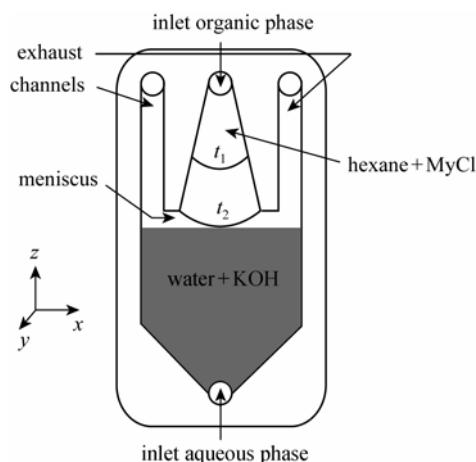


Figure 2 Principal sketch of the experimental system [The solid lines in the organic phase refer to the meniscus positions at different time (t_1, t_2) during the filling]

The convective patterns are visualized by a high-resolution shadowgraph system (TSO, Pulsnitz, Germany) with a CCD camera (Dalsa 2M30-SA, 1600×1200 pixel, frame rate of 10fps), which is mounted on an optical bench. As normal, experiments are conducted in a vertical HS cell ($\alpha \rightarrow 0$), *i.e.* gravity vector acts parallel to the plates. The angle dependence is determined by carrying out experiments with the optical bench tilted by an angle, α , relative to the vertical line (see Fig. 3).

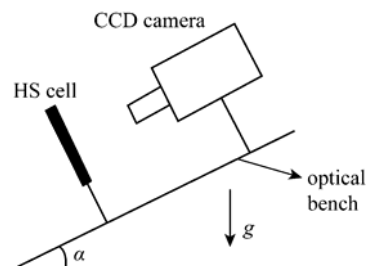


Figure 3 Scheme of the experimental setup

The velocity fields are obtained using digital particle image velocimeter (PIV). Polystyrene particles

(density $1.02\text{g}\cdot\text{ml}^{-1}$, diameter $9.9\mu\text{m}$), which turned out to be suitable for being chemically inert, are added into the aqueous phase. The illumination is either in the front (vertical HS cell) or from below (horizontal HS cell) by means of a standard slide projector. To reduce the heat input, two heat adsorption filters are employed. The particle motion is recorded by a CMOS camera (NOBLE-Kamerawerke, 256×512 pixel) with a frame rate of 50 fps. It is switched to a zoom macro-scope, allowing for different size of object field.

3 RESULTS AND DISCUSSION

The most striking feature of this system is a mode transition, *i.e.* depending on the tilting angle of the HS cell, different sorts of Marangoni instabilities occur.

3.1 Chemo-Marangoni cells ($\alpha\rightarrow 0$)

If the Hele-Shaw cell is placed in a vertical position (g in the direction of $-z$), a pattern of chemo-Marangoni cells is observed aligned along the interface. These roll cells grow very fast. Within two minutes the number of the cells is reduced during the reaction to three or two larger roll cells. A characteristic feature of these cells is the vigorous dynamics emanating from the stagnation points which oscillate in both vertical and horizontal direction. It seems that the reaction takes place preferably at these points. Associated with the "wave" is the production of some small-scale Marangoni cells (first order), which are advected into the center of the already existing second order cells. Fig.4 displays the shadowgraph pictures which represent the evolution of chemo-Marangoni cells in a vertical Hele-Shaw cell.

These phenomena are observable from 15 to 60min depending on C_{M0} and C_{B0} . In the shadowgraph pictures (see Fig.4) roll cells can only be seen in the aqueous phase due to the precipitation and emulsion in the organic phase, but in fact they exist on both phases, which can be revealed by PIV method. Fig.5 presents the characteristic velocity field obtained from PIV. It can be easily detected that the cells appear on both phases in pair. A series of PIV experiments is conducted in order to determine the velocity scale, which leads to the result that the characteristic veloc-

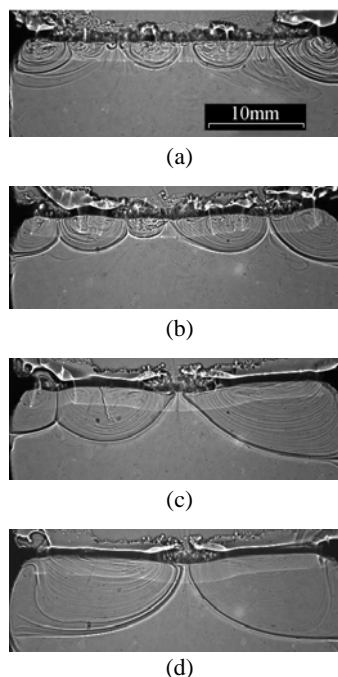


Figure 4 Evolution of chemo-Marangoni cell pattern in a vertical Hele-Shaw cell for $C_{M0}=0.4\text{mol}\cdot\text{L}^{-1}$ and $C_{B0}=0.2\text{mol}\cdot\text{L}^{-1}$ at time (a) $t=50\text{s}$; (b) $t=75\text{s}$; (c) $t=100\text{s}$; (d) $t=170\text{s}$ after the start of the reaction

ity in this system is in the range of $0.5\text{--}3\text{mm}\cdot\text{s}^{-1}$ depending on the absolute initial concentrations. With higher concentrations, velocity is larger and accompanied with the faster growth of the roll cells.

3.2 Large scale interfacial deformation ($\alpha\rightarrow 90^\circ$)

If the same reaction system is studied when the Hele-Shaw cell is placed in a horizontal position, *i.e.* Hele-Shaw cell oriented perpendicular to the vector of gravitational acceleration, large scale interfacial deformations, periodic in space and time, coupled with Marangoni convection, are observed.

Immediately after the start of the reaction, typical, nice Marangoni cells can be clearly seen in the aqueous phase accompanied by the small-amplitude (0.5mm) deformations with short wavelength [see Fig.6(a)].

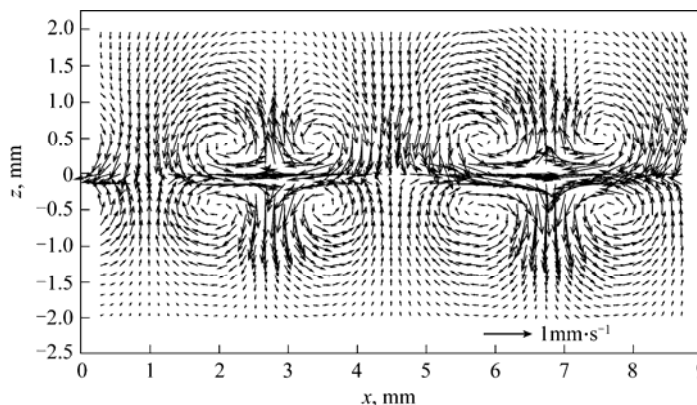


Figure 5 Typical velocity field showing chemo-Marangoni cells in a vertical Hele-Shaw cell for $C_{M0}=0.2\text{mol}\cdot\text{L}^{-1}$ and $C_{B0}=0.15\text{mol}\cdot\text{L}^{-1}$ at $t=60\text{s}$

With the growing time, the wavelength increases in parallel with the larger amplitude. For example, in Fig.6(b), after 35s of the start of the reaction, the wavelength increases around 3 times while the amplitude of the deformations reaches 2mm. However, these two stages continue only for short time (40s), then the system crosses over to a time-periodic interfacial deformation in form of a few “noses” (the regular deformation is named here after nose), which eject from the organic phase toward the aqueous one, see Fig.6(c).

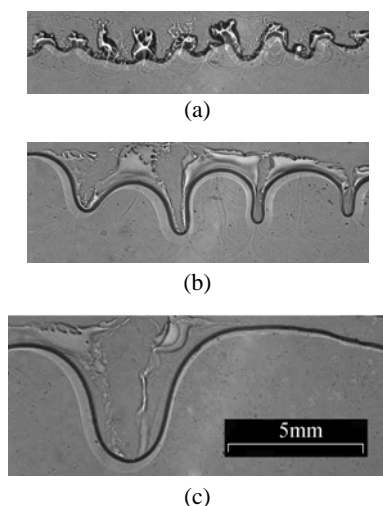


Figure 6 Interfacial deformations in a horizontal Hele-Shaw cell for $C_{M0}=0.2\text{mol}\cdot\text{L}^{-1}$ and $C_{B0}=0.1\text{mol}\cdot\text{L}^{-1}$ at time (a) $t=4\text{s}$; (b) $t=35\text{s}$; (c) $t=165\text{s}$ after the start of the reaction
(Lower phase corresponds to the aqueous phase while the upper layer organic phase)

Now we focus our discussion on the periodicity of the interfacial deformation. As a whole, the interface deforms advancing into the aqueous phase and then recedes. External Marangoni convection in the aqueous phase becomes distinct and further promotes the nose receding [see Fig.6(b)]. The flow inside the Marangoni cells directs towards the interface at the cell margins, *i.e.* at the nose formation places, and away from the interface in the cell center, which is illustrated in Fig.7.

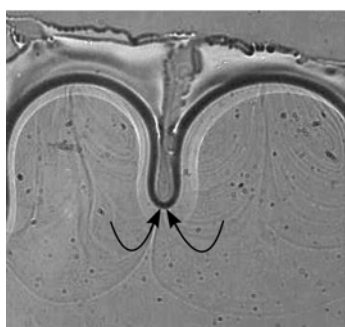


Figure 7 Nose receding promoted by the external Marangoni convection and the flow inside Marangoni cells is shown with the arrow

In Fig.8(a) we analyze the deformation of the interface, characterized by the distance H between the

interface and the nose tip as a function of time for the case $C_{M0}=0.3\text{mol}\cdot\text{L}^{-1}$ and $C_{B0}=0.1\text{mol}\cdot\text{L}^{-1}$, and the corresponding velocity v , dH/dt is plotted in Fig.8(b). Based on the figures, it can be clearly found that the interfacial deformation happens periodically with the lifetime 4s while the maximum deformation reaches 9mm. Moreover, the nose advances with the velocity $16\text{mm}\cdot\text{s}^{-1}$, then it goes back with a much smaller velocity $7\text{mm}\cdot\text{s}^{-1}$. Finally it enters into a slower recovery process to prepare for the next sudden burst. This process is similar to a spring accumulating the energy and releasing suddenly. Compared with the characteristic Marangoni velocity ($1\text{mm}\cdot\text{s}^{-1}$), nose advancement velocity is approximately 10 times faster. However, the lifetime of the nose, intensity and nose velocity depend on the gap width and absolute initial concentrations. Basically with the increase of the gap width, the deformation magnitude decreases while the frequency increases. And the advancement velocity decreases, becoming comparable with the receding one.

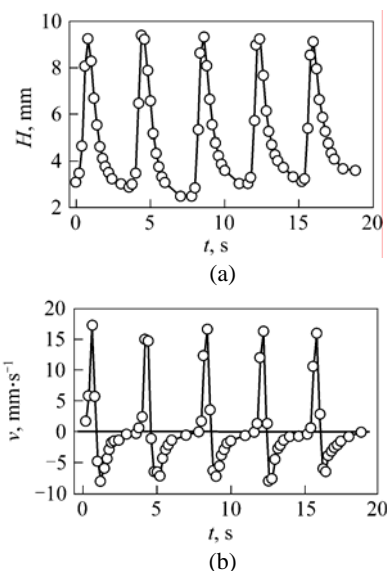


Figure 8 Deformation of the interface (a) and corresponding velocity (b) as a function of time for $C_{M0}=0.3\text{mol}\cdot\text{L}^{-1}$ and $C_{B0}=0.1\text{mol}\cdot\text{L}^{-1}$

3.3 Roll cells+interfacial deformations ($0 < \alpha < 90^\circ$)

If we tilt the Hele-Shaw cell with a definite angle ($0 < \alpha < 90^\circ$) toward the horizontal position, the pattern will lead to a combination of interfacial deformation and roll cells. Fig.9 displays such kind of instability with the help of the tracer particles for two different tilting angles. In the pictures, the white in the organic phase represents the precipitation of the product due to its lower solubility. In Fig.10 the corresponding velocity fields are given, in which only the velocity in the aqueous phase are drawn while $z=0$ refers to the original interface position.

If we compare the two cases: the tilting angle $\alpha=15^\circ$ and $\alpha=75^\circ$, it can be detected that with the increase of the tilting angle α , *i.e.* gravity influence is reduced, the roll cells become weaker while the deformation of the stagnation points normal to the interfaces are intensified. The deformation for the case $\alpha=$

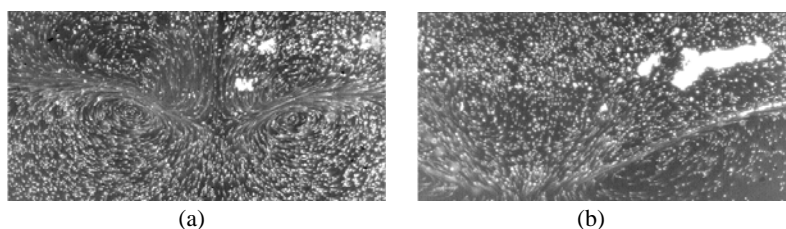


Figure 9 Combination of interfacial deformation and cellular mode with tracer particles in a Hele-Shaw cell with the tilting angle (a) $\alpha=15^\circ$; (b) $\alpha=75^\circ$
(lower layer refers to the aqueous phase while upper layer organic phase)

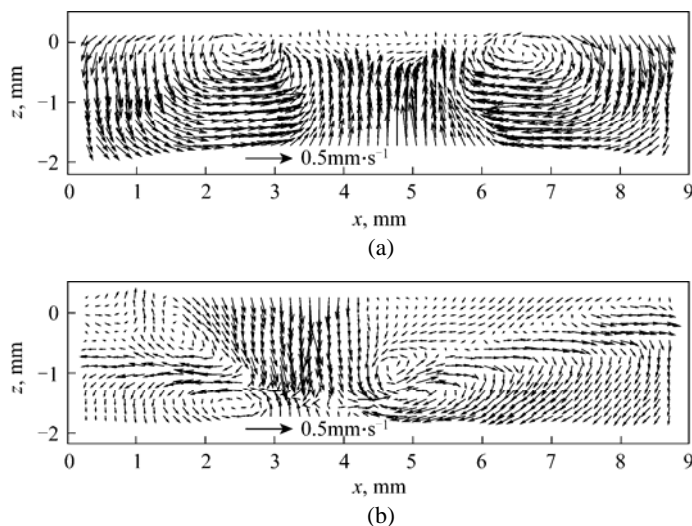


Figure 10 Corresponding velocity field for the above two cases
($z=0$ refers to the original interface position)

15° is around 0.5mm , and the typical roll cell structure can be clearly seen [Fig.10(a)]. However, for the case $\alpha = 75^\circ$ [Fig.10(b)], the roll cells become much weaker than in the former case while the deformation of the interface approaches 1.5mm , which becomes the dominant instability.

3.4 Discussion

Through the chemical reaction an *in situ* surfactant (here potassium myristate) is produced. It is adsorbed at the interface, leading to a reduction of the interfacial tension. The main phenomena which the surfactant undergoes are: adsorption-desorption process and partition of the surfactant since the P-My is soluble in both phases. And there is a strong interaction with the hydrodynamics.

The difference between vertical and horizontal position of a Hele-Shaw cell may be qualitatively discussed. In the vertical position, due to the interfacial tension gradient caused by the *in situ* produced surfactant, Marangoni convection is initiated. Meanwhile, buoyancy arising from the unstable density stratification reinforces such vigorous Marangoni convection. There is a competition between convection and adsorption preventing larger interfacial deformation. As a result, the oscillations normal to the interface present of much smaller amplitude.

In the horizontal position, the relative influence of gravity is reduced. The surfactant has enough time

to get adsorbed at the interface leading to the drastic reduction of interfacial tension. Thus the force balance at the triple junction, $F = \sigma_{os} - \sigma_{ws} - \sigma \cos \theta$ (see Fig.11) is disturbed resulting in the change of contact angle θ at the glass plates and the creation of shear stress both parallel and perpendicular to the HS-plates. Here σ_{os} and σ_{ws} are the interfacial energies at the organic-solid and aqueous-solid interfaces, σ is the interfacial tension between organic and aqueous phases. By virtue of the shear stress parallel to the plates, a strong internal circulation inside the organic phase (at the low- σ -place) develops which pushes the organic phase into the aqueous one, giving rise to the nose spreading phenomenon. Then owing to the large increase in surface area and partial surfactant desorption, which causes the increase of the interfacial tension in vicinity of nose tip, the nose growth is stopped. In parallel, since the shear stress is reduced, the transport of fresh chemicals is interrupted,

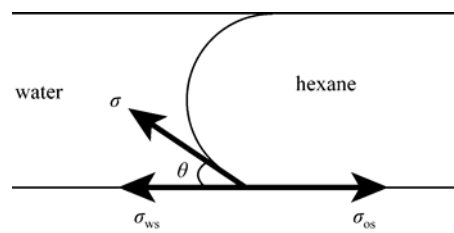


Figure 11 Forces at the triple junction from the side view of y direction

which is followed by the fact that not enough surfactants are produced to sustain the gradient of interfacial tension. Therefore, the driving forces break down and the nose receding sets in. Nose relaxation is further promoted by the external Marangoni convection (see Fig.7) via the normal stress balance. In addition, the desorption of the surfactant is also assisted by such convection. After that it will take some time for the diffusion of the reactants to build up the necessary critical gradients to start a new further cycle.

4 CONCLUSIONS

The object of study was an immiscible liquid-liquid system placed in a Hele-Shaw cell, in which an interfacial reaction takes place leading to an *in situ* production of surface active substances. Depending on the tilt angle of the Hele-Shaw cell, different kinds of Marangoni instabilities occur.

If the Hele-Shaw cell is oriented in a vertical position, a pattern of chemo-Marangoni cells is observed with the typical velocity ($1\text{mm}\cdot\text{s}^{-1}$). A characteristic feature of these cells is the vigorous oscillation of their stagnation points in both vertical and horizontal directions. However, oscillation normal to the interface is of much smaller amplitude than that in horizontal Hele-Shaw cell position.

By tilting the Hele-Shaw cell toward a horizontal position the cellular mode becomes weaker while the oscillation of the stagnation points normal to the interface is intensified. With the increase of the tilting angle, the deformation of the interface becomes more dominant instability.

Finally in a horizontal Hele-Shaw cell, the chemical system can be characterized by several remarkable features, such as spontaneous large scale interfacial deformation with a spatio-temporal periodicity and vivid chemo-Marangoni convection. The local decrease of interfacial tension changes the contact angle at the solid plates resulting in the force imbalance at the contact line. In addition, it also creates a shear stress parallel and perpendicular to the plates, which together with the force imbalance causes the spreading phenomena.

ACKNOWLEDGEMENTS

We thank Margret Acker, Armin Heinze for numerous fruitful discussions.

NOMENCLATURE

C	molar concentration, $\text{mol}\cdot\text{L}^{-1}$
g	gravity acceleration, $\text{m}\cdot\text{s}^{-2}$
H	interface deformation, mm
t	time, s
v	velocity, $\text{mm}\cdot\text{s}^{-1}$
α	tilting angle, ($^{\circ}$)
ν	kinematic viscosity, $\text{m}^2\cdot\text{s}^{-1}$
ρ	density, $\text{kg}\cdot\text{m}^{-3}$
σ	interfacial tension, $\text{mN}\cdot\text{m}^{-1}$

Subscripts

B	base species (KOH)
M	myristoyl chloride
o	organic phase
s	solid (glass)
w	aqueous phase

0 initial state

REFERENCES

- Ma, Y.G., Yang, X.W., Feng, H.S., Yu, G.C., "Influence of interfacial turbulence on gas-liquid mass transfer", *Chem. Eng. (China)*, **32**, 1—4(2004). (in Chinese)
- Sha, Y., Cheng, H., Yu, Y.H., "The numerical analysis of the gas-liquid absorption process accompanied by Rayleigh convection", *Chin. J. Chem. Eng.*, **10**, 539—544(2002).
- Ma, Y.G., Feng, H.S., Xu, S.C., Yu, G.C., "The mechanism of interfacial mass transfer in gas absorption process", *Chin. J. Chem. Eng.*, **11**, 227—230(2003).
- Warmuzinski, K., Buzek, J., "A model of cellular convection during adsorption accompanied by chemical reaction", *Chem. Eng. Sci.*, **45**, 243—254(1990).
- Sherwood, T.S., Wei, J.C., "Interfacial phenomena in liquid extraction", *Ind. Eng. Chem.*, **49**, 1030 (1957).
- Ermakov, S.A., Ermakov, A.A., Chupakhin, O.N., Vaisov, V.V., "Mass transfer with chemical reaction in conditions of spontaneous interfacial convection in processes of liquid extraction", *Chem. Eng. J.*, **84**, 321—324 (2001).
- Calves, J.Y., Danes, F.E., Gentric, E., Lijour, Y., Sanfeld, A., Saumagne, P., "Spontaneous turbulence induced by interfacial reactions", *J. Colloid Interface Sci.*, **129**, 130—138(1989).
- Hughes, M.A., "On the direct observation of films formed at a liquid-liquid interface during the extraction of metals", *Hydrometallurgy*, **3**, 85 (1978).
- Nakache, E., Dupeyrat, M., Lemaire, J., "Enhanced recovery of metals by liquid-liquid extraction: Influence of the interfacial properties of the extractant", *J. Chem. Phys.*, **83**, 339 (1986).
- Shioi, A., Kumagai, H., Sugiura, Y., Kitayama, Y., "Oscillations of interfacial tension and spontaneous interfacial flow at a water/oil interface composed of Di(2-ethylexyl) phosphoric acid", *Langmuir*, **18**, 5516 (2002).
- Avnir, D., Kagan, M.L., "The evolution of chemical patterns in reactive liquids, driven by hydrodynamic instabilities", *Chaos*, **5**, 589—601(1995).
- Nakache, E., Duperat, M., Vignes-Adler, M., "Experimental and theoretical study of an interfacial instability at some oil-water interfaces involving a surface-active agent", *J. Colloid Interface Sci.*, **94**, 187 (1983).
- von Gottberg, F.K., Hatton, T.A., Smith, K.A., "Surface instabilities due to interfacial chemical reaction", *Ind. Eng. Chem. Res.*, **34**, 3368—3379(1995).
- Kai, S., Ooishi, E., Imasaki, M., "Experimental study of nonlinear waves in interface between two liquid phases with chemical reaction", *J. Phys. Soc. Jpn.*, **54**, 1274—1287(1985).
- Kai, S., Müller, S., Mori, T., Miki, M., "Chemically driven nonlinear waves and oscillations at an oil-water interface", *Physica D*, **50**, 412—428(1991).
- Fernandez, J., Homsy, G.M., "Viscous fingering with chemical reaction: effect of *in situ* production of surfactants", *J. Fluid Mech.*, **480**, 267—281(2002).
- Linde, H., Kunkel, M., "Einige neue qualitative Beobachtungen beim oszillatorischen Regime der Marangoni-Instabilität", *Warme- und Stoffübertrag.*, **2**, 60 (1969).
- Eckert, K., Grahn, A., "Plumes and finger regimes driven by an exothermic interfacial reaction", *Phys. Rev. Lett.*, **82**, 4436—4439(1999).
- Eckert, K., Acker, M., Shi, Y., "Chemical pattern formation driven by a neutralization reaction. I. Mechanism and basic features", *Phys. Fluids*, **16**(2), 385—399(2004).
- Shi, Y., Eckert, K., "Acceleration of reaction fronts by hydrodynamic instabilities in immiscible systems", *Chem. Eng. Sci.*, **61**, 5523—5533(2006).
- Shi, Y., Eckert, K., Heinze, A., Acker, M., "The chemically driven interfacial convection (CDIC)-Experiments on MASER 10", In: 17th ESA Symposium on European Rocket and Balloon Programmes and Related Research, Sandetjrd, Norway (2005).